Comprehensive analysis of 3D & 2D model of MoS_2

Written by:

Kristoffer Varslott

Department of Physics UiO

UNIVERSITY OF OSLO

November 25, 2019

Contents

I Introduction **3**

II Comprehensive DFT-analysis **4**
i Creation of MoS_2 Slab 4
ii Convergence of cut-off energy and **k**-points densities 5
iii Electronic Density of states & Band structure 7

III Numerical results **9**
i Bulk structure of MoS_2 [2H] 9
ii Monolayer MoS_2 [2H] 10

IV Discussion **11**
i Band structure 11
ii Electronic Density of States 11
iii Calculated bandgap [E_g] vs experimental value 11

V Conclusion **12**

Abstract

Analysing MoS_2 using DFT calculations with GGA functional provides an inaccurate approximation to experimental data of the bandgap of bulk and monolayer [1.29eV][1.90eV], respectivly [1] [2]. Where the bandgap for bulk was calculated to 0.93eV, whit a relative error $\epsilon_{rel} = 27.9\%$, and for monolayer bandgap of 1.62eV with $\epsilon_{rel} = 14.2\%$. Looking at both bulk and thin layer MoS_2, it was discovered that the band structures for these two structures differed quite a lot. Where the bulk MoS_2 gave a indirect bandgap and the thin layer MoS_2, showed a direct bandgap.

I. Introduction

Molybdenum sulphides has a so-called isotypic crystal structure and is classified as transition metal dichalcogenide. In this paper, one will investigate both bulk and monolayer structures of MoS_2 2H. This kind of arrangement of molybdenum sulphide is trigonal prismatic, which means that the sulphides is arranged in a symmetric order above and underneath the molybdenum atom.

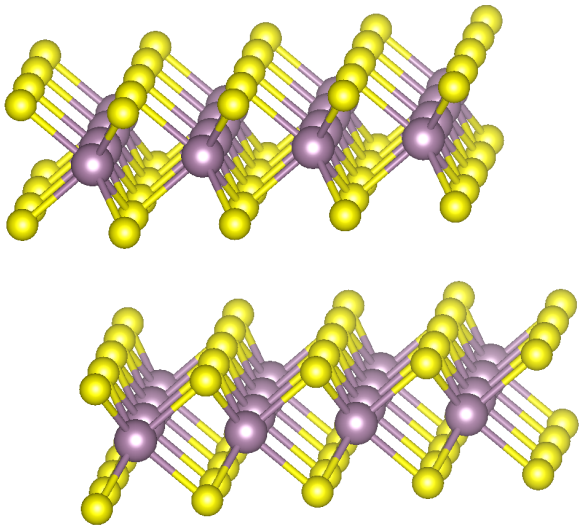

Figure 1: Illustration of the bulk MoS_2 2H. Where the yellow illustrates the sulphides and purple molybdenum atoms

MoS_2 occurs naturally in nature as molybdenite. in its bulk form, as we will investigate, it appears as a dark, shiny solid. The bulk layer sheets is held up by weak Van der Waals forces. These forces is the holding stone of the bulk solid. In bulk form it is often used as a lubricant, due to its weak interlayer forces. As for the thin layer MoS_2, we extrapolate the layer of the bulk MoS_2. We will investigate which properties that change as we go from bulk to thin layer film. By looking at density of states for both systems and investigating the band structures. Further more when analysing MoS_2, we will use standardize self-consistent calculation method in which the Hartree Fock method is applied.

The transition metal dichalcogenide [MoS_2] is known for its electrical properties as well as its optoelectronic properties. The bulk MoS_2 has a indirect bandgap of 1.29eV [1], while the monolayer MoS_2 has a direct bandgap of 1.90eV [2].

II. Comprehensive DFT-analysis

In this section there will be a brief but comprehensive description on how the results where manifested. The DFT-analysis where done on two materials. Bulk and monolayer MoS_2, which consist of 6 and 3 atoms in the desired supercell. The fact that the supercell consisted of a small number of atoms, our DFT-calculations where minimized with respect to computational power.

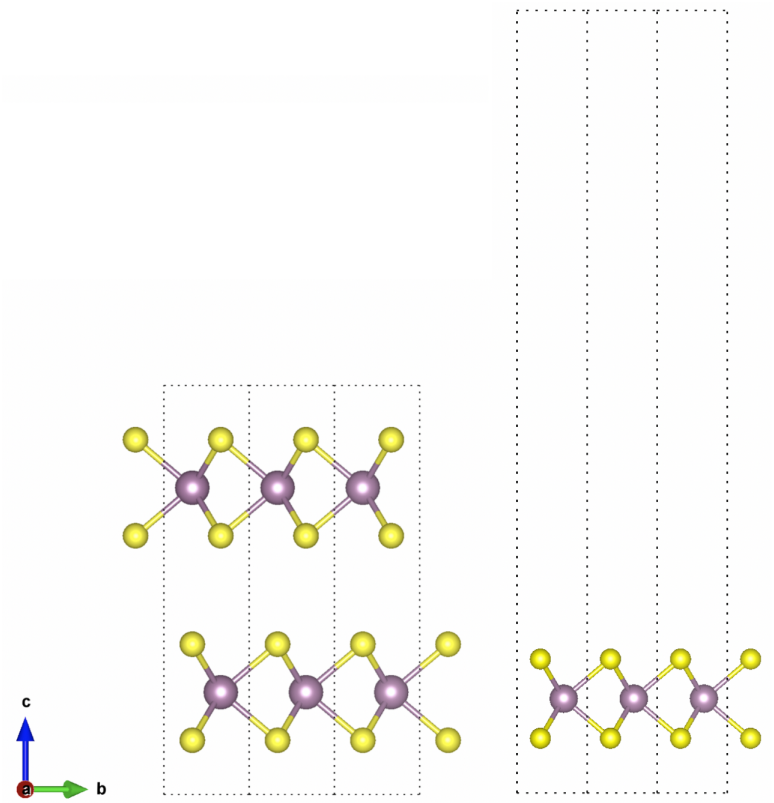

Figure 2: Visualization of MoS_2 2H - bulk (left) and the slab (right). Supercells is defined within the stippled lines.

As we can see the by figure 2, Slab contains quite different length in the c-direction. A vacuum layer of of 12Å where inserted to reduce interlayer interactions due to Van der Waals forces. The POSCAR file[1], contain structural information on the material MoS_2. Once we have established which structure to work on, we need to start our DFT calculations. One commonly starts with Cut-off energy and K-points density. It is important to have sufficient cut-off energy and K-points densities before starting the calculations. Before diving in to this, we first need to take a closer look at how to create the slab.

i. *Creation of MoS_2 Slab*

In able to get a good approximation of a 2D-material one need to insert a vacuum layer in the material, to distance the interlayer in the bulk. A self-consistent DFT calculation where done here, by inserting a vacuum layer in the c-direction. Gradually increasing the vacuum layer with 2Å per calculation. In the INCAR-file the tag IVDW = 1 where inserted. This tag takes care of the Van

[1] `https://materialsproject.org/materials/mp-2815/`

der Waals forces in between the layers. The main object here, is to see when the total energy is converged.

Listing 1: Initial POSCAR-file for bulk

```
MoS2
 1.0000000000000000
     3.1903157300000000    0.0000000000000000    0.0000000000000000
    -1.5951578649999993    2.7628944682730965    0.0000000000000000
     0.0000000000000000    0.0000000000000000   14.8790043000000001
  Mo   S
   2   4
Direct
  0.3333330000000000  0.6666670000000000  0.2500000000000000
  0.6666670000000001  0.3333330000000000  0.7500000000000000
  0.3333330000000000  0.6666670000000000  0.8551740000000000
  0.6666670000000001  0.3333330000000000  0.1448260000000000
  0.6666660000000000  0.3333330000000000  0.3551739999999999
  0.3333340000000000  0.6666670000000000  0.6448260000000000
```

Listing 1 the POSCAR-file for bulk MoS_2 2H is shown, where for creation of slab one increase the c-direction with a vacuum layer.

Table 1: Inserted vacuum layer in c-direction in POSCAR file, with corresponding energies

Vacuum layer [Å]	**E_{tot} [eV]**
2	-22.356
4	-22.355
6	-22.354
8	-22.355
10	-22.355
12	-22.355

Table 1, gives a good convergence of energies as vacuum layer is increased. In this analysis a vacuum layer of 12Å where used for further calculations to ensure no interlayer interactions. Once the slab has been created, the convergence test of cut-off energy and **k**-points density may be established.

ii. *Convergence of cut-off energy and* **k***-points densities*

This subsection will contain information on cut-off energy and K-points density convergence tests. The convergence test is done by checking the relative total energy of bulk and slab. Energy cut-off is an important parameter in DFT-calculations. One need a large energy cutoff in order to reproduce the wavefunction to some desired accuracy. The cut-off energy contains many k-points, which all represent a plane wave.

$$\psi_{\mathbf{k}}(\mathbf{r}) = u_{\mathbf{k}}(\mathbf{r})e^{i\mathbf{k}\cdot\mathbf{r}} \tag{1}$$

Where $u_{\mathbf{k}}(\mathbf{r})$ is a bloch function which describes the periodic potential in the crystal. The periodicity of the bloch function means that it can be represented as a set of plane waves that spans the reciprocal space:

$$u_{\mathbf{k}}(\mathbf{r}) = \sum_{\mathbf{G}} c_{\mathbf{G}} e^{i\mathbf{G}\cdot\mathbf{r}} \tag{2}$$

$$\psi_{\mathbf{k}}(\mathbf{r}) = \sum_{\mathbf{G}} c_{\mathbf{k}+\mathbf{G}} e^{i(\mathbf{k}+\mathbf{G})\cdot\mathbf{r}} \tag{3}$$

Where $\mathbf{G}$ is the vector defined by $\mathbf{G} = m_1\mathbf{b_1} + m_2\mathbf{b_2} + m_3\mathbf{b_3}$ These waves is being combined in the calculations to represent the wavefunction. In order to represent the wavefunction one need a sufficient amount of plane-waves, however, an unlimited E_{cutoff} is unrealistic since it needs an unlimited amount of computing power.

$$E = \frac{\hbar^2}{2m}|\mathbf{k} + \mathbf{G}| \rightarrow E_{cut} = \frac{\hbar^2}{2m}G_{cut}^2 \tag{4}$$

Which further yields a constraint to equation 3:

$$\psi_{\mathbf{k}}(\mathbf{r}) = \sum_{|\mathbf{k}+\mathbf{G}|<G_{cut}} c_{\mathbf{k}+\mathbf{G}} e^{i(\mathbf{k}+\mathbf{G})\cdot\mathbf{r}} \tag{5}$$

Therefore we do a convergence test on cut-off energies to see which energy cut-off is sufficient.

Table 2: Convergence of total energy of both bulk and slab as a function of energy cutoff, also relative energy of bulk and slab

$\mathbf{E_{cutoff}}$ [eV]	$\mathbf{E_{tot}}$ [bulk] [eV]	$\mathbf{E_{tot}}$ [slab] [eV]	$\mathbf{E_{rel}}$ [eV]
250	-44.865	-22.352	-22.513
300	-44.908	-22.373	-22.535
350	-44.929	-22.384	-22.545
400	-44.936	-22.387	-22.549
450	-44.937	-22.388	-22.549
500	-44.938	-22.388	-22.549

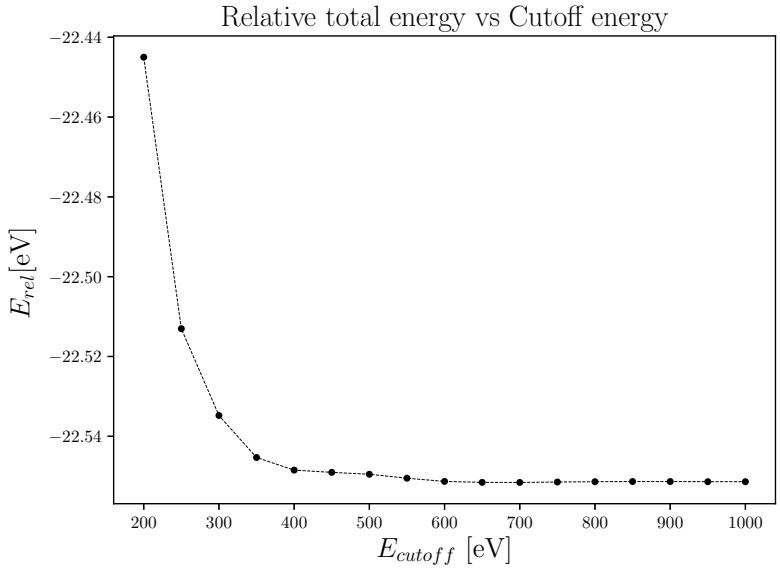

Figure 3: Number of k-points needed for a given ENCUT. If the dimension of the unitcell diminishes in one direction, the **k**-mesh gets smaller.

k-mesh is the integration points in our calculations. If our unit cell is large in one direction we need a small **k**-point in that direction. for small unit-cells we need a high **k**- mesh in order to

[2]In the directory: ∼olem/fm4111/bin/makekpoints

produce the results with high enough accuracy. Giving an accurate density and total energy of the system. By this the number of integration points is altered as we insert a vakuum layer. For the bulk structure the python-file makekpoints -d #density^2 where used as well as for the monolayer structure. Choosing the appropriate **k**-mesh is vital for accurate calculations.

Table 3: Convergence of **k**-points density as a function of total energy, and relative energy of bulk and slab.

k-points	$\mathbf{E_{tot}}$ **[bulk] [eV]**	$\mathbf{E_{tot}}$ **[slab] [eV]**	$\mathbf{E_{rel}}$ **[eV]**
2	-45.043	-22.442	-22.601
3	-44.935	-22.386	-22.549
4	-44.937	-22.387	-22.549
5	-44.937	-22.388	-22.550
6	-44.937	-22.388	-22.550
7	-44.937	-22.388	-22.550

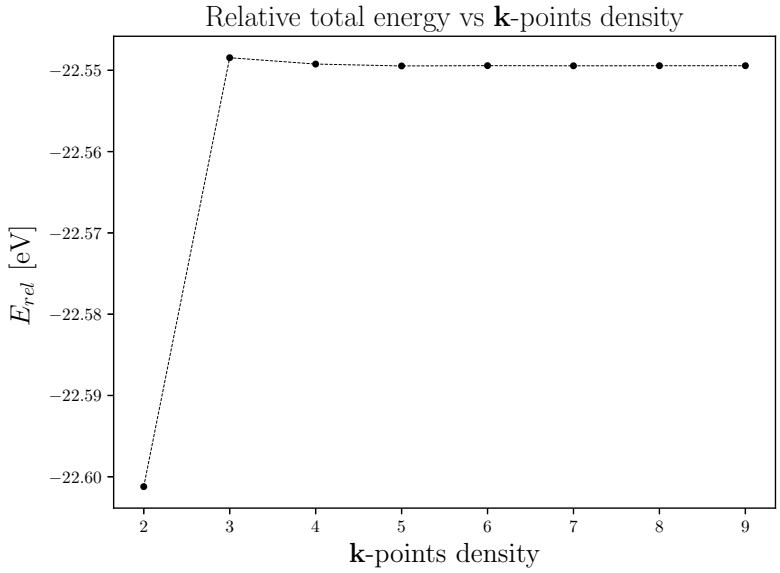

Figure 4: Number of k-points needed for a given ENCUT. If the dimension of the unitcell diminishes in one direction, the **k**-mesh gets smaller.

As we can see by table 3 and figure 4 the convergency rapidly occurs as the KPOINTS denisty is increased. For calculations a **k**-point density of 5 was submitted. This gave sufficient convergence when the relative total energy where analysed. When it comes to the mesh-points for a thinlayer structure it is sufficient to set **k**-mesh to one in the direction where the vakuum layer is being implemented.

iii. *Electronic Density of states & Band structure*

In this section we will undergo a brief study of relaxation of the structure before going forwards with density of states and band structure. To relax the bulk structure was demanding. Problems occurred during the iterations, towards relaxing the structure. The fact that the energies diverged at

some point was troubling. Managed to overcome this problem, by readjusting the lattice vector in the c-axis. Small change gave an easy relaxation of the structure. Relevant tags in the INCAR file was:

The relaxation was done on both the ions and the unitcell. Where the IBRION = 1 tag is used to relax the ions into their instantaneous groundstate. However, the problem may have been that the initial position guess was not suitable for IBRION = 1. By setting IBRION = 2 we got a satisfactory answer, where the structure was relaxed without further implications. Once the structure was relaxed, one can calculate the density of state and band structure.

Density of states was calculated using NSW = 0, a static self-consistent calculation. Used DOSCAR to plot the density of state as a function of E $[eV]$. In order to get an accurate representation of density of state (DOS), one needed to use a large number of k points. The reason is that when calculating DOS one analyses the integrals in k-space, a more compact k-mesh gives a more accurate description of the integrals.

$$\bar{g} = \frac{V_{cell}}{(2\pi)^3} \int_{BZ} g(\mathbf{k}) d\mathbf{k} \tag{6}$$

Previously in our calculation a k-mesh of $10 \times 10 \times 3$ for bulk and $10 \times 10 \times 1$ for monolayer. With k-density of 5. By increasing the number of k-points to $24 \times 24 \times 6$ and for monolayer $24 \times 24 \times 1$, with k density of 12. We where able to get a more accurate description of DOS.

When calculating the band structure, the same k-mesh was used. The first calculations done where self-consistent calculations using PAW PBE potential with GGA functional, the produced CHGCAR file was then used to calculate the band structure. The next step was to alter the KPOINTS-file to contain the symmetry path of k-points. By this we needed to understand how the Brillouin zone for a hexagonal structure was structured.[3]

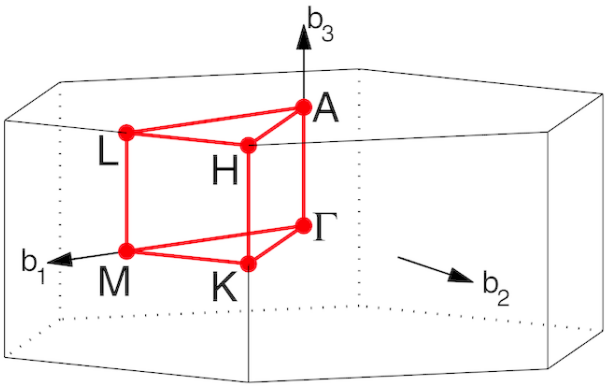

Figure 5: Illustration of Brillouin zone in hexagonal lattice with irreducible Brillouin zone marked in red line

Figure 5 show the Brillouin zone as well as the high-symmetry path. These k points paths where written into the KPOINTS-file. The full high-symmetry path is as follows: $\Gamma - M - K - \Gamma - A - L - H - A|L - M|K - H$, however, the path was reduced to $\Gamma - M - K - \Gamma$ in this text. This is because the area of interest lies within this region. We also need to add the tag ICHARG = 11 in order to read the CHGCAR file.

[3]Figure 5 is taken from the article
High-throughput electronic band structure calculations: Challenges and tools [3]

III. Numerical results

This section will present results regarding the bulk MoS_2 as well as the monolayer MoS_2. The electronic density of state for both cases will be presented, and the resulting band structures. The plots where possible due to the scripts [plotbands.py, dosplot.py], which where available through the directory: ∼olem/fm4111/bin. Alternation of the py-files has been done, in order to match up with the given structure at hands.

i. *Bulk structure of MoS_2 [2H]*

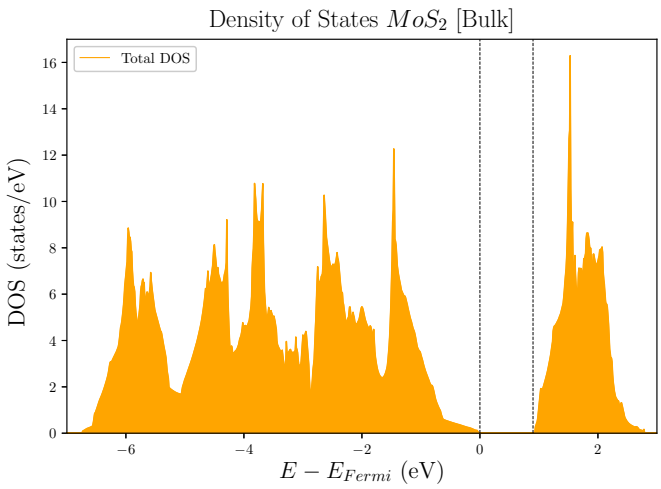

Figure 6: Electronic density of states (DOS) of MoS_2 [bulk], as calculated by VASP using PAW-PBE potential with GGA functional. Where the dashed lines indicates the bandgap.

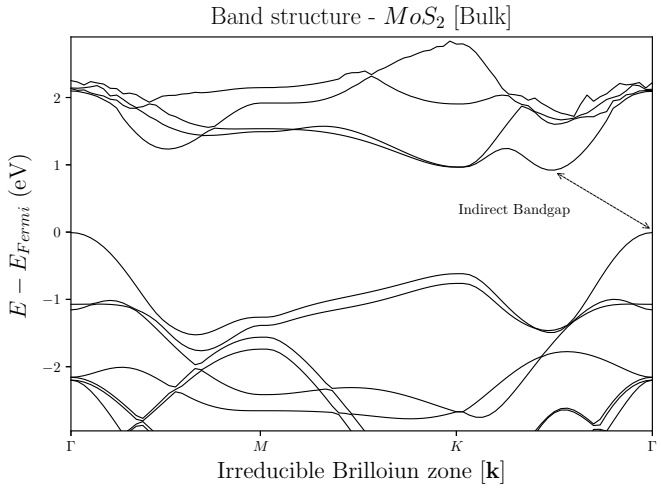

Figure 7: Band structure of bulk MoS_2, showing an indirect bandgap at high symmetry point Γ, with 30 points from one symmetry point to another.With bandgap calculated to $E_g = 0.93$

ii. *Monolayer MoS_2 [2H]*

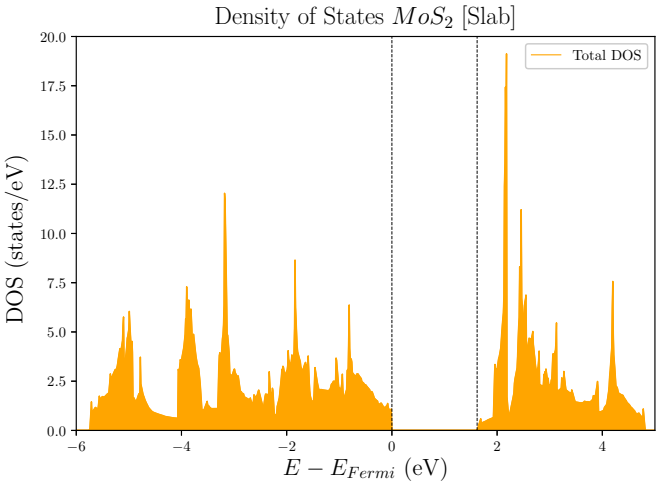

Figure 8: Electronic density of states (DOS) of MoS_2 [Slab], as calculated by VASP using PAW-PBE potential with GGA functional.Where the dashed lines indicates the bandgap.

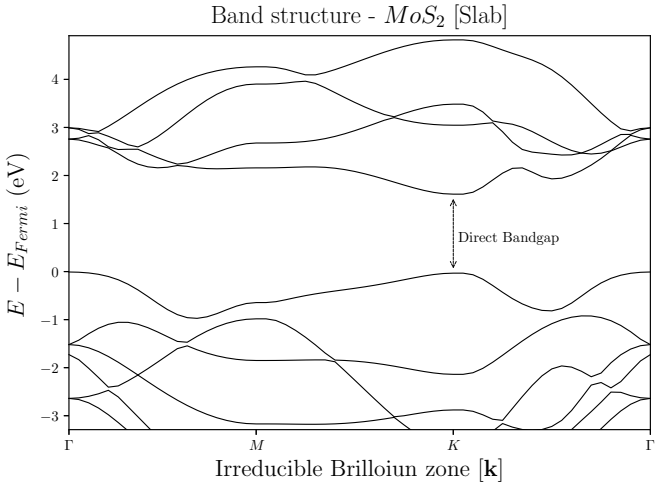

Figure 9: Band structure of monolayer MoS_2, showing a direct bandgap at high symmetry point K, with 20 points from one symmetry point to another. With bandgap calculated to $E_g = 1.62$

IV. Discussion

i. *Band structure*

The main goal of this article was to investigate the alternation of band structure from bulk to monolayer MoS_2, as well as look at the given electronic density of states in both cases. As we can see by figures 7,9. The bulk exhibits an indirect bandgap, at the Γ centre point, while the monolayer exhibits a direct bandgap at the symmetry point K. The shift of bandgap location is interesting, as one can see there is clearly a shift going from a bulk to monolayer structure. Some explanation may be that when the structure is in bulk, the monolayers is interacting with each other through Van der Waals forces, the symmetry and geometry of the crystal is different from the single monolayer structure. The most important reason for a change is what happens when we look at the monolayer, it experience a so-called quantum confinement effect, this is because the particles size in the c-direction is to small to be comparable with the electron wavelength. As the dimension is decreased we get discrete energy levels $\epsilon_{n,z}$, where n is the quantum number. So this discretization of energy levels in the z-direction(equivalent to c-direction), gives a shift from Γ-centered valence band to K-centered valence band. For the indirect bandgap, there is needed a change in momentum in order to transition the electron from valence band to conduction band. This change in momentum mostly comes from phonon contribution. For the direct bandgap, there is no need for change in momentum, as long as the photon has energy near the bandgap energy E_g, it can excite the electron up to the conduction band, and an emission of photon may take plays.

ii. *Electronic Density of States*

Figures 6 shows the electronic density of states for bulk. The DOS gives an calculation of number of electron states within a interval $E, E+dE$, where it is plotted as a function of $E - E_{fermi}(eV)$, At E $= E_{fermi}$, and the region where $E < E_{fermi}$ we see the valence band. The region where the density of states is zero theres a bandgap. The stippled line at $E - E_{fermi} = 0.93eV$, and above shows the conduction band. As we can see, there is a small amount of electron states at the valence band maxima and conduction band minima for the bulk. At zero kelvin $T = 0K$, there is no electrons in the conduction band due to fermi-dirac statistics. At zero kelvin the fermi-function acts as a step-function, where all electron is populated in the valence band, where as no electron has sufficient energy to be in the conduction band. 8, shows the electronic density of states for the monolayer. A clear distinction between figure 6 and 8 is that there is a higher number of states occupied near the valence band maxima for the monolayer. Tracing back to the discussion about direct bandgap, we can see that there is a chance that more electron will occupy near the valence band maxima, yielding a higher order of photon emission. Another interesting property of monolayer MoS_2 is that as a photon excites an electron to the conduction band a hole is created in the valence band, yielding an existing exciton (electron-hole par). As the electron and hole is seperated, they create an electrical current in the crystal, which is one of the fundamental properties of a semiconductor. Finally by looking figures 6 and 8, observe some sharp peaks, which a is discontinuously change in the slope of DOS. These discontinuities is characterized as Hove singularities [4].

iii. *Calculated bandgap [E_g] vs experimental value*

The Bandgap estimated by VASP, was calculated to to 0.93eV for bulk MoS_2, which is dramatically underestimated compared to the experimental value of 1.29eV, [1]. For the monolayer it was calculated to 1.62eV compared to the experimental value of 1.90eV [2]. The calculation done by VASP is as we see roughly underestimates the bandgap for both cases. As standard DFT-calculations

using a GGA functional fails to correctly estimate the electronic states near the fermi energy. Relative error is calculated below for bulk case, with E_g being the calculated bandgap from VASP and $E_{ex,g}$ being the experimental bandgap.

$$\epsilon_{rel} = \frac{|E_g - E_{ex,g}|}{E_{ex,g}} \times 100\% = \frac{|0.93eV - 1.23eV|}{1.23eV} \times 100\% = 27.9\% \tag{7}$$

Relative error of bandgap for monolayer MoS_2:

$$\epsilon_{rel} = \frac{|E_g - E_{ex,g}|}{E_{ex,g}} \times 100\% = \frac{|1.62eV - 1.90eV|}{1.90eV} \times 100\% = 14.2\% \tag{8}$$

A better way of calculating the bandgap is to use hybrid functionals, one example is HSE06, which provides a better estimate of the bandgap for small bandgap semiconductors. As we see the bandgap of bulk is much narrower than that for monolayer. This can be explained by the decrease of dimension in the c-direction. As the dimension is decreases we reach reach a discretization of energy levels as mentioned above, this increases the the size of the bandgap.

V. Conclusion

The bulk and monolayer MoS_2 band structures and electronic density of states where calculated, and showed a clear transition from indirect to direct bandgap. The monolayer structure is therefore more suitable for photonic devices, due to no momentum change in $\mathbf{k}$. The bandgap calculated was grossly underestimated compared to the experimental value. This underestimation is due to the choice of functional, if the calculations had been done using a hybrid functional such as HSE06 functional the results would probably coincide with the experimental values. The GGA functional managed described the shape of the band structure and electronic density of states. The bandgap where align along a high symmetry point, which is fairly normal. The transition of bandgap symmetry point alignment could be described though the minimisation of the dimension along c-direction.

References

[1] Changgu Lee, Hugen Yan, Louis E Brus, Tony F Heinz, James Hone, and Sunmin Ryu. Anomalous lattice vibrations of single-and few-layer mos2. *ACS nano*, 4(5):2695–2700, 2010.

[2] Kin Fai Mak, Changgu Lee, James Hone, Jie Shan, and Tony F Heinz. Atomically thin mos 2: a new direct-gap semiconductor. *Physical review letters*, 105(13):136805, 2010.

[3] Wahyu Setyawan and Stefano Curtarolo. High-throughput electronic band structure calculations: Challenges and tools. *Computational materials science*, 49(2):299–312, 2010.

[4] David Sholl and Janice A Steckel. *Density functional theory: a practical introduction*. John Wiley & Sons, 2011.